MELBA Journal Machine Learning for Biomedical Imaging

GIM-ENDO: A Multimodal Endoscopic Image and Video Dataset for Gastric Intestinal Metaplasia Morphology and Pathology

Mojgan **Forootan** [1], Mahziar **Setayeshfar** [2], Ali **Darvishi** [3], Mohammad **Tashakoripour** [4], Hamidreza **Bolhasani** [5,*]

1 Shahid Beheshti University of Medical Sciences, Tehran, Iran
2 Iran University of Medical Sciences, Tehran, Iran
3 Shiraz University of Medical Sciences, Shiraz, Iran
4 Tehran University of Medical Sciences, Tehran, Iran
5 DataBioX Research, Tehran, Iran

Abstract

Gastric intestinal metaplasia (GIM) is a histopathologically confirmed precursor to gastric adenocarcinoma. Early, accurate detection remains a clinical challenge, and AI-assisted endoscopy is a promising solution. We present **GIM-ENDO**, a publicly available multimodal dataset comprising 98 endoscopic still images and 39 video clips from 24 patients (22 GIM-positive, 2 normal controls), acquired with the Olympus EVIS X1 system under white-light endoscopy (WLE), narrow-band imaging (NBI), and magnifying NBI (M-NBI). All cases are histopathologically confirmed. Annotations cover six IEE endoscopic signs (LBC, MTB, WOS, TV pattern/Fusion, atrophy, MLE), GIM subtype (complete/incomplete), and OLGA/OLGIM staging where available. The dataset is publicly accessible at `https://doi.org/10.5281/zenodo.20707267`. For the latest updates, refer to `https://databiox.com`.

Keywords

Gastric Intestinal Metaplasia; Image-Enhanced Endoscopy; Narrow-Band Imaging; Artificial Intelligence; Deep Learning; Endoscopic Dataset; OLGA; OLGIM

Article informations

`https://doi.org/10.59275/j.melba.2026-86cc`
Volume 2026, Received: 2026-06-19, Published 2026-09-21
Corresponding author: * hamidreza@databiox.com
Special issue: MICCAI Open Data 2026 x MELBA
Guest editors: AT, MS et al.

1. Background

Gastric cancer accounts for approximately 1.1 million new cases and 769,000 deaths annually, ranking as the fifth most common malignancy and the fourth leading cause of cancer death worldwide (Sung et al., 2021). The majority of gastric adenocarcinomas arise through the Correa cascade: normal mucosa → chronic gastritis → atrophic gastritis → intestinal metaplasia → dysplasia → carcinoma (Correa, 1992). GIM represents the first irreversible step and substantially elevates cancer risk, particularly in the incomplete subtype (González et al., 2020; Wang et al., 2023).

AI-assisted image-enhanced endoscopy (IEE) has emerged as a promising complement to clinical practice. Deep learning systems approach or exceed expert accuracy for gastrointestinal lesion detection (Hirasawa et al., 2018; Mori et al., 2018), and GIM-specific studies demonstrate encouraging performance with IEE (Dohi et al., 2020; Martins et al., 2025). However, clinical translation remains constrained by the scarcity of openly accessible, annotated, multimodal datasets with histopathological validation, IEE-sign annotations, and normal mucosal controls.

1.1 Related Resources

Few public datasets integrate histopathologically validated GIM with detailed IEE-sign annotations, standardized grading, and normal controls in a single resource. Yang et al. (2023) released 21,493 WLE/linked-colour-imaging images for binary IM/atrophy classification, without IEE-sign characterisation. GastroHUN (Bravo et al., 2025) offers 8,834 images across 22 anatomical landmarks, without GIM-specific labels. HyperKvasir (Borgli et al., 2020) covers broad gas-

Table 1: Comparison of GIM-related public datasets.

Dataset	Pub.	N	Sub.	IEE	OLGA
Yang et al. (Yang et al., 2023)	✓	21k	–	–	–
Ligato et al. (Ligato et al., 2024)	✓	1,384	–	–	–
Fang et al. (Fang et al., 2024)	–	2,725	✓	–	✓
GastroHUN (Bravo et al., 2025)	✓	8,834	–	–	–
HyperKvasir (Borgli et al., 2020)	✓	110k+	–	–	–
GIM-ENDO (Ours)	✓	99	✓	✓	✓

Pub.: publicly available; N: number of images; Sub.: GIM subtype; IEE: IEE-sign annotations; OLGA: OLGA/OLGIM staging.

trointestinal findings without dedicated GIM labeling. Table 1 summarises these resources.

1.2 Novelty

GIM-ENDO is, to our knowledge, the first public multimodal dataset combining histopathological validation, expert IEE-sign annotation (LBC, MTB, WOS, TV pattern, MLE, atrophy), GIM subtype labeling, OLGA/OLGIM staging, and normal mucosal controls in a single resource. The dataset supports AI tasks aimed at improving targeted biopsy, endoscopic resection planning, and early interruption of the carcinogenesis cascade.

2. Summary

2.1 Vision and Objectives

GIM-ENDO is designed to enable AI models capable of real-time GIM detection and characterization from IEE data. Key objectives are: (1) extraction of discriminative endoscopic features (WOS, LBC, MTB, TV pattern, atrophy, MLE); (2) binary GIM classification and complete/incomplete subtype prediction; and (3) automated OLGA/OLGIM risk staging to support clinical decision-making worldwide.

2.2 AI Readiness

Data are provided in standard formats (JPEG, PNG, MP4) with consistent file naming that encodes anatomical location, modality, and annotated features. All metadata and per-image/per-case annotations (endoscopic features, GIM subtype, OLGA/OLGIM stage, *H. pylori* status) are stored in a structured Excel (`.xlsx`) file linked to media files via unique identifiers. No predefined train/validation/test split is included, allowing flexible, task-specific partitioning.

2.3 Resources Needed

The dataset is accessible at `https://doi.org/10.5281/zenodo.20707267`. Standard Python libraries (NumPy, Pandas, OpenCV, PyTorch, TensorFlow) are sufficient for data loading and model development. Given the current dataset size (≈98 images, 39 video clips), experiments can be run on CPU-based systems; GPU use is optional.

Table 2: Demographic and pathological characteristics.

Characteristic	GIM+	Control
N (patients)	22	2
Images / Videos	92 / 34	6 / 5
Age, Median (IQR)†	59 (55–68)	N/A
Sex, Female N (%)	14 (63%)	1 (50%)
H. pylori +, N (%)	4 (20%)	—
Complete GIM	8	—
Incomplete GIM	7	—
Complete + Incomplete	3	—
Subtype Unconfirmed	4‡	—
OLGA I–II	5	—
OLGA III–IV	1	—
OLGA Not Assessed	16§	—

† Age/sex missing for 1 patient (2617). ‡ GIM-positive, subtype not further classified (patients 2609, 2617, 2618). § Incomplete biopsy-site sampling in 15/21 cases.

Table 3: IEE endoscopic signs in GIM-positive cases (patient level).

Sign	GIM+ ($N = 22$)
LBC (Light Blue Crest)	16 / 22 (73%)
MTB (Marginal Turbid Band)	5 / 22 (23%)
WOS (White Opaque Substance)	4 / 22 (18%)
TV pattern (Fusion)	12 / 22 (55%)
TM (Transparent Mucosa)	14 / 22 (64%)
MLE (Map-like Erythema)	5 / 22 (23%)

3. Methods

3.1 Data Details

Consecutive adults (≥18 years) undergoing upper GI endoscopy for dyspepsia, screening, or surveillance were prospectively enrolled across multiple centers. Exclusion criteria: prior gastric surgery, history of gastric malignancy, active upper GI bleeding, or inadequate biopsy samples. Demographic and pathological characteristics are in Table 2.

Table 3 shows the distribution of IEE endoscopic signs at patient level.

3.2 Methods Used for Data Creation

All procedures used the Olympus EVIS X1 system (processor: CV-1500). Gastroscopes were CF-EZ1500DL (primary) and CF-H190L (subset). Modalities: WLE, M-NBI, and NBI with near focus. Still images: JPEG/PNG at 2879×1799 px (full-frame) and 657×454 px (near-focus). Videos: MP4, 30 fps, ≈50 s, 1920×1080 px. Each anatomical location (antrum, body/corpus, incisura angularis, prepy-

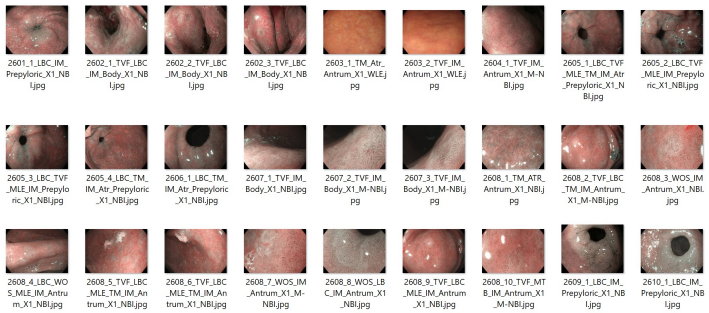

Figure 1: Representative endoscopic images from the GIM-ENDO dataset. File names encode anatomical location, modality, and detected features (e.g., LBC, WOS, TV pattern).

Demographics				Endoscopic Findings (Image/Video)							Pathology		
Case Code	Media Type	Age	Sex	LBC	MTB	WOS	TVF	IRV	MLE	TM	Histological Subtype	Atrophy	Dysplasia
2601	Image	64	Female	Prepyloric	Negative	Negative	Negative	Negative	Negative	Negative	Incomplete (Prepyloric)	N/A	Negative
2602	Image	69	Male	Body	Negative	Negative	Body	Negative	Negative	Negative	Complete + Incomplete (Body)	Body	Negative
2603	Image	67	Female	Negative	Negative	Negative	Antrum	Negative	Negative	Antrum	Complete (Antrum)	Antrum	Negative
2604	Image	58	Female	Negative	Negative	Negative	Antrum	Negative	Negative	Negative	Complete (Antrum)	Antrum	Negative
2605	Image	62	Female	Prepyloric	Negative	Negative	Prepyloric	Negative	Prepyloric	Prepyloric	Incomplete (Prepyloric)	Prepyloric	Negative
2606	Image	57	Female	Prepyloric	Negative	Negative	Negative	Negative	Negative	Prepyloric	Complete (Prepyloric)	Prepyloric	Negative
2607	Image	86	Female	Negative	Negative	Negative	Body	Negative	Negative	Negative	Complete (Antrum)	Antrum	Negative
2608	Image	67	Male	Antrum	Antrum	Antrum	Antrum	Negative	Antrum	Antrum	Complete (Antrum/Prepyloric)	Prepyloric	Negative
2609	Image	59	Female	Prepyloric	Negative	Negative	Negative	Negative	Negative	Negative	IM Positive	Negative	Negative
2610	Image & Video	45	Male	Prepyloric	Prepyloric	Prepyloric	Body	Negative	Negative	Prepyloric	Incomplete (Prepyloric)	Prepyloric	Negative
2611	Image	67	Female	Antrum	Negative	Negative	Antrum	Negative	Antrum	Antrum	Complete + Incomplete (Antrum)	Negative	Negative
2612	Image	71	Female	Antrum	Antrum	Antrum	Antrum	Negative	Negative	Antrum	Complete + Incomplete (Antrum / Antrum - Incisura)	Antrum - Incisura	LGD / Antrum
2613	Image	56	Male	Antrum	Both	Prepyloric	Antrum	Negative	Antrum	Negative	Incomplete (Antrum/Prepyloric)	Negative	Negative
2614	Image	39	Male	Prepyloric	Negative	Negative	Negative	Negative	Negative	Negative	Incomplete (Prepyloric)	Prepyloric	Negative
2615	Image	68	Male	Antrum	Negative	Negative	Antrum	Negative	Negative	Antrum	Incomplete (Antrum)	Antrum	Negative

Figure 2: Structured annotation and metadata file (XLSX). Columns include demographics, IEE findings (LBC, MTB, WOS, TV pattern, MLE, TM), and histopathological outcomes (GIM subtype, atrophy, dysplasia).

loric region) was documented as both a still image and a video clip.

The initial release contains 137 samples (98 still images, 39 video clips), all histopathologically confirmed. Suspicious lesions prompted targeted biopsies per the updated Sydney Protocol (Dixon et al., 1996); confirmed cases were recorded and annotated by experienced advanced endoscopists. The file naming convention encodes anatomical location, modality, and detected IEE features (e.g., LBC, WOS, TV pattern), facilitating structured traceability.

4. Validation

4.1 Quality Control and Ground-Truth Verification

All files were inspected for completeness, correct anatomical labeling, and absence of identifiable information prior to inclusion. Ground truth was established through four steps: (i) targeted biopsies per updated Sydney Protocol; (ii) independent histological assessment by two board-certified GI pathologists; (iii) expert annotation by multiple advanced endoscopists with standardized IEE-sign definitions; and (iv) consensus-based resolution of discordant cases. Cases without complete biopsy-site coverage were excluded from definitive OLGA staging and flagged in the annotation file.

4.2 Annotation Consistency

Standardized definitions were applied consistently. Formal inter-rater and intra-rater reliability were not assessed in this pilot release (acknowledged as a limitation in Section 5.2). Users should note that MTB and TV-pattern subcategories are inherently subject to inter-observer variability.

4.3 Benchmark Protocol

No predefined data split is provided, allowing task-specific partitioning (e.g., patient-level). Supported tasks include binary GIM detection, subtype classification (complete vs. incomplete), per-sign detection, and OLGA/OLGIM staging. Evaluation metrics (e.g., AUROC, sensitivity at fixed specificity) should be chosen according to the intended clinical application.

5. Discussion

5.1 Strengths

GIM-ENDO is clinically grounded and systematically annotated, integrating multimodal endoscopic data (WLE, M-NBI, NBI), histopathological confirmation, and structured metadata. Unlike prior datasets relying solely on static images, the inclusion of video clips provides a richer representation of mucosal dynamics. The fine-grained annotation of six IEE signs supports both binary GIM detection and advanced per-feature classification, enabling interpretable AI systems aligned with clinical practice.

5.2 Limitations and Biases

The primary limitation is modest sample size in this initial release (98 images, 39 videos). Normal control cases are limited owing to the high prevalence of *H. pylori* and environmental risk factors in the studied population. Formal inter-/intra-rater reliability was not assessed. Rare OLGA/OLGIM stages (III–IV) and the incomplete GIM subtype are underrepresented. Future releases will expand cohort size, add multi-center data, and include multi-expert consensus annotation.

5.3 Responsible Use

GIM-ENDO is intended for non-commercial research only. Models must not be deployed clinically without independent prospective validation. Re-identification attempts, commercial use, and surveillance applications are strictly prohibited under the CC BY-NC 4.0 license (`https://creativecommon org/licenses/by-nc/4.0/`).

6. Resource Availability

GIM-ENDO is publicly available at `https://doi.org/10.5281/zenodo.20707267`. The repository contains 98 still images (JPEG/PNG), 39 video clips (MP4/MKV), and anonymised clinical metadata in a structured `.xlsx` file. All files use consistent naming conventions; media–metadata linkage is via unique identifiers.

Target ML tasks: binary GIM detection; subtype classification (complete vs. incomplete); per-sign detection (LBC, MTB, WOS, TV pattern, atrophy, MLE, AHP, GA); OLGA/OLGIM staging. **Clinical domain:** upper GI endoscopy for premalignant lesion screening and risk stratification. **License:** CC BY-NC 4.0. For the latest updates, visit `https://databiox.com`.

Acknowledgments

Not applicable.

Ethical Standards

This study was approved by the ethics committee of the Gastroenterology and Liver Disease Research Center, Research Institute for Gastroenterology and Liver Diseases, Shahid Beheshti University of Medical Sciences (Ethics Approval No.: IR.SBMU.RIGLD.REC.1405.039). All data are fully anonymised. Informed consent was obtained from all participants and/or their legal guardians.

Conflicts of Interest

The authors declare no competing financial or non-financial interests.

Data availability

GIM-ENDO is openly available at `https://doi.org/10.5281/zenodo.20707267`. The repository contains endoscopic still images (JPEG/PNG), video clips (MP4/MKV), and anonymised clinical metadata (XLSX) including *H. pylori* status and all IEE-sign annotations. Access is open and unrestricted.

References

H. Borgli, V. Thambawita, P.H. Smedsrud, et al. HyperKvasir, a comprehensive multi-class image and video dataset for gastrointestinal endoscopy. *Sci Data*, 7(1): 283, 2020. .

D. Bravo, J. Frias, F. Vera, et al. GastroHUN: a multiclass gastrointestinal endoscopy dataset. *Sci Data*, 12:102, 2025. .

P. Correa. Human gastric carcinogenesis: a multistep and multifactorial process. *Cancer Res*, 52(24):6735–6740, 1992.

M.F. Dixon, R.M. Genta, J.H. Yardley, et al. Classification and grading of gastritis: the updated Sydney System. *Am J Surg Pathol*, 20(10):1161–1181, 1996.

O. Dohi, N. Yagi, A. Majima, et al. Diagnostic ability of AI using deep learning of magnifying NBI for gastric intestinal metaplasia. *Dig Endosc*, 32(2):255–263, 2020. .

S. Fang, Z. Liu, Q. Qiu, et al. Semi-supervised deep learning for intestinal metaplasia and gastric atrophy on pathological images. *Gastric Cancer*, 27(4):701–713, 2024.

C.A. González, J.M. Sanz-Anquela, J.P. Gisbert, et al. Utility of subtyping intestinal metaplasia as a marker of gastric cancer risk. *Eur J Cancer Prev*, 29(5):391–397, 2020.

T. Hirasawa, K. Aoyama, T. Tanimoto, et al. Application of deep learning for gastric cancer detection. *Gastric Cancer*, 21(4):653–660, 2018. .

I. Ligato, G. De Magistris, E. Dilaghi, et al. CNN model for intestinal metaplasia recognition from BLI images. *Diagnostics*, 14(13):1376, 2024. .

M.L. Martins, M. Dinis-Ribeiro, M. Coimbra, and F. Renna. Predicting endoscopic grading of gastric intestinal metaplasia using small patches. *IEEE EMBC*, 2025.

Y. Mori, S.E. Kudo, M. Misawa, et al. Real-time use of AI in identification of diminutive polyps during colonoscopy. *Ann Intern Med*, 169(6):357–366, 2018. .

H. Sung, J. Ferlay, R.L. Siegel, et al. Global cancer statistics 2020: GLOBOCAN estimates. *CA Cancer J Clin*, 71 (3):209–249, 2021. .

Z. Wang, L. Li, J. Wang, et al. Incomplete intestinal metaplasia is a risk factor for gastric cancer: a cohort study. *Gastric Cancer*, 26(2):189–201, 2023. .

J. Yang, Y. Ou, Z. Chen, et al. Benchmark dataset for intestinal metaplasia and gastritis atrophy. *IEEE J Biomed Health Inform*, 27(1):7–16, 2023. .